Scanning tunneling microscopy of laser-activated carbon electrodes used in studies of electrochemical charge-transfer reactions

R. S. Robinson[a)]
Bellcore, Navesink Research and Engineering Center, 3Z-275, Red Bank, New Jersey 07701

Kent Sternitzke and Richard L. McCreery[a)]
Department of Chemistry, The Ohio State University, Columbus, Ohio 43210

(Received 24 July 1990; accepted 26 October 1990)

Carbon electrodes form the basis of a variety of electroanalytical sensors, in part due to their low cost, wide potential range, and suitability for modification. A major research effort is underway in many laboratories to understand better the properties of carbon electrodes regarding electrocatalytic activity and other factors such as background current and electron transfer activity. One method of improving the performance of these electrode materials involves the application of pulses from a Nd:YAG or N_2 laser, either during or prior to electrochemical use. Both electrochemical and spectroscopic probes indicate dramatic changes to the surface of the electrodes after the pulses. Raman spectroscopy of the electrode surface indicates damage to the carbon lattice, with an increase in intensity of the Raman band at 1360 cm^{-1}. This band is active in crystallites of finite size, and indicates increased exposure of graphitic edge plane. Also, there is a dramatic increase ($\geqslant 10^6\times$) in heterogeneous charge-transfer rates measured with redox benchmark probes [$Fe(CN)_6^{-3/-4}$, dopamine]. Mechanisms of electrode activation by the laser pulses can involve roughening of the electrode surface, or ablation or cleaning of the electrode. Scanning tunneling microscope (STM) images of graphite and glassy carbon surfaces before and after delivery of laser pulses of various energies show a roughening of the surface from the laser treatment, with the appearance of new features of submicron size. The graphite electrodes show a highly disrupted surface, with jagged features and high roughness factors, determined from the STM images. None of the types of features observed in the laser-activated regions of graphite electrodes have been previously observed in our laboratory, in the course of dozens of experiments involving the imaging of different samples and grades of fresh or mechanically damaged graphite electrodes.

I. INTRODUCTION

Highly oriented pyrolytic graphite (HOPG) has been studied by several groups as an electrode material, due mainly to its well defined surface structure compared to more commonly used materials such as glassy carbon (GC). The basal plane of HOPG is also a common standard for scanning tunneling microscopy (STM) because it is atomically flat over regions up to at least 10^4 A^2, and is generally free of gross microstructural defects. Thus HOPG serves well as a nearly perfect single-crystal surface for studies of the chemical properties of basal plane sp^2 carbon.

A major research effort is underway in many laboratories to better understand the properties of carbon electrodes regarding background current and electron transfer activity. The basal plane of HOPG has an anomalously low capacitance in electrolytic solution compared to typical metals and edge plane carbon.[1-3] The heterogeneous electron transfer rate at HOPG is strongly dependent on the presence of graphitic edge plane for several redox systems, with the rate constant on edges being $\sim 10^5$ times that on basal plane.[1,4,5] These observations indicate the electrochemical importance of defects on HOPG and by implication to a variety of graphite materials. However, because electrochemical methods depend on the spatial average of the surface on a distance scale much larger than the defects, the surface morphology of HOPG and laser damaged HOPG was investigated at the STM level.

II. EXPERIMENTAL

The STM used was described previously.[6-8] The *xyz* translator was a bend-polarized tube with a coaxially mounted tube for *z* translation. Images were recorded with the scanner moving in both directions of the *x* and *y* scans. The images shown here have been corrected for scanner creep;[9] the amount of correction varied with the scan area, from 2 to 15% for scans from 400 nm to 4.5 μm. A 32-bit microcomputer (Apple Macintosh II with MacAdios II interface, GW Instruments) and two (640 by 480 and 1024 by 768 pixels) 256-color monitors were used for STM control and image display. The scanning wave form generation circuit[10] dynamically optimized the scan rate for surface roughness,[6] minimizing image acquisition time on surfaces with a wide range of roughness. The scanning and image display software allowed a large-area survey scan to be performed, with interactive zooming to an area of interest.[11] The tip bias for all images was + 55 mV and the tunneling current 2–3 nA (constant-current mode.) The tips were made from 250 μm Pt wire (Longreach Scientific, Pt-010-30-R). The graphite samples were type "ZYA" HOPG (Union Carbide, Parma, Ohio).

 0734-211X/91/020960-04$01.00

The details of the voltammetry and Raman spectroscopic measurements are reported elsewhere.[1,4] $Fe(CN)_6^{-3/-4}$ voltammetry was conducted in 2 M KCl. Laser activation with a Nd:YAG (1064 nm) laser was carried out in air as described previously[1,4] at both 55 and 105 MW cm^{-2} as noted below. A small N_2 laser (337 nm) was also used in several cases, with the beam attenuated by metal apertures and focused onto the HOPG with a 10× microscope objective.[12] The N_2 laser activation averaged 67 MW cm^{-2} over a ~22 μm radius spot.

III. RESULTS AND DISCUSSION

A series of gray-scale images of the surface of ZYA-grade HOPG, taken to establish baseline conditions, are shown in Fig. 1. The gray shading is keyed to tip displacement; all features in the images were stable over a 24 h observation period. Figure 1(A) shows a typical step defect that appears on HOPG. Figure 1(B) shows a double ridge which appears to emanate from a step defect. The ridges vary between 5 and 30 Å high, and are each 100 Å across. Figures 1(C) and 1(D) are layers of graphite, folded into a ribbon-like structure. The types of features shown in Figs. 1(B)–1(D) are less common but illustrate some examples of the variety of structures that occur on HOPG. Images of glassy carbon (Tokai GC-20) are shown in Fig. 2. The sample shown in Fig. 2(A) has been polished sequentially with 1, 0.3, and 0.05 μm alumina grit; scratches from the polishing procedure are visible. Figures 2(B)–2(D) are of the freshly exposed electrode surface, after fracturing the electrode.

Electrochemical characteristics of HOPG ZYA basal plane are shown in Fig. 3. Curves 1 and 2 are cyclic voltammograms for dopamine and $Fe(CN)_6^{-3/-4}$. The curve shapes, particularly the separation of the oxidation and reduction waves, indicate the electrochemical charge transfer rate. Voltammetry curves for noble metal (Pt, Au, Pd) electrodes for dopamine and $Fe(CN)_6^{-3/-4}$ usually resemble those of curves 3 and 4, but because of slow charge transfer at

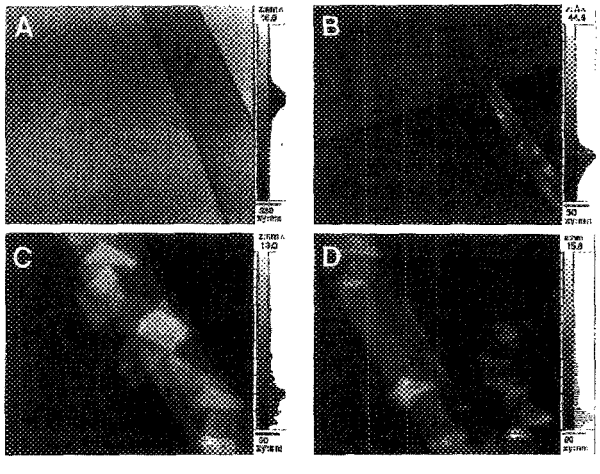

FIG. 1. STM images of HOPG basal plane. The lateral ($X-Y$) scale is given at the lower right of each panel. The Z-axis range is given at the top right of each panel; the curve to the right of the gray scale is a histogram of the proportion of pixels in the image which represent a given tip displacement.

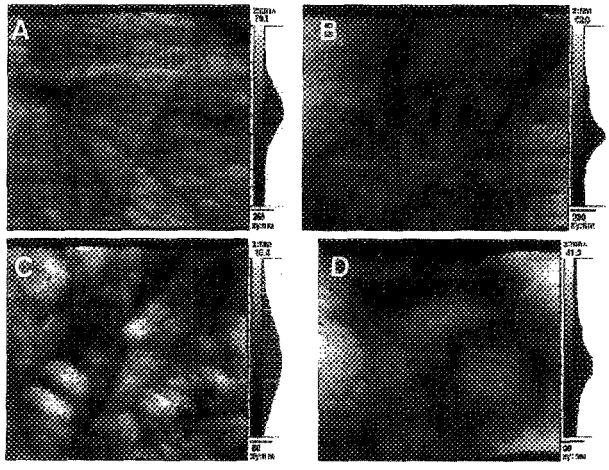

FIG. 2. STM images of a glassy carbon electrode. (A) is after polishing with 1, 0.3, and 0.05 μm alumina. (B), (C), and (D) are of a freshly exposed surface produced by fracturing the electrode.

HOPG basal plane the shapes of curves 1 and 2 are distorted. The observed heterogeneous rate constant k^0_{obs} for $Fe(CN)_6^{-3/-4}$, calculated from the voltammogram, is $< 10^{-9}$ cm/s; in contrast, after applying three 50 MW cm^{-2} laser pulses, k^0_{obs} improves dramatically to 1.8×10^{-3} cm/s. The laser-treated surface shows a more moderate (factor of ~30) increase in capacitance in electrolytic solution;[13] but the increased rate constant is not simply a consequence of increased electrode surface area, but of increased edge plane density; k^0_{obs} of the laser-treated surface agrees with published data for the magnitude of k^0_{obs} on native edge plane.[5]

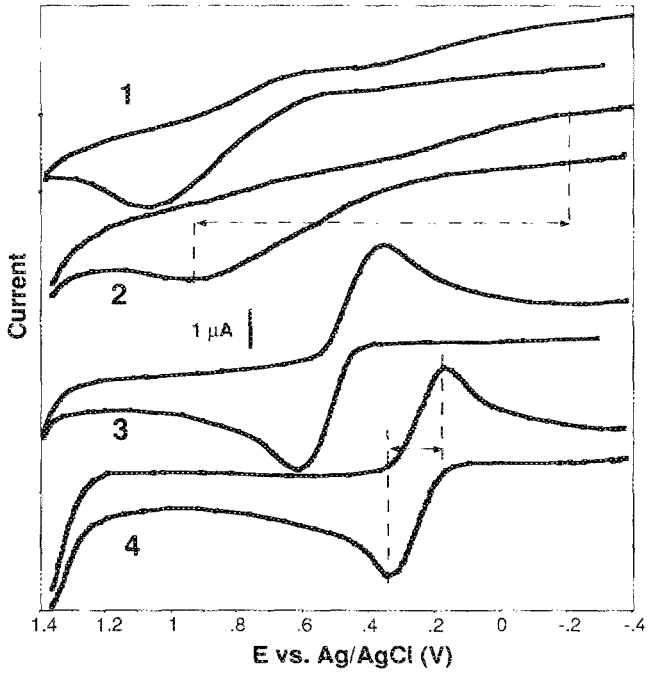

FIG. 3. Cyclic voltammograms of dopamine (0.1 M H_2SO_4) (1,3) and $Fe(CN)_6^{-3/-4}$ (1 M KCl) (2,4) on HOPG. The scan rate was 0.2 V s^{-1}. Curves 1 and 2 were on untreated, and curves 3 and 4 laser treated (50 MW cm^{-2}, three pulses) HOPG. Adapted from Ref. 4.

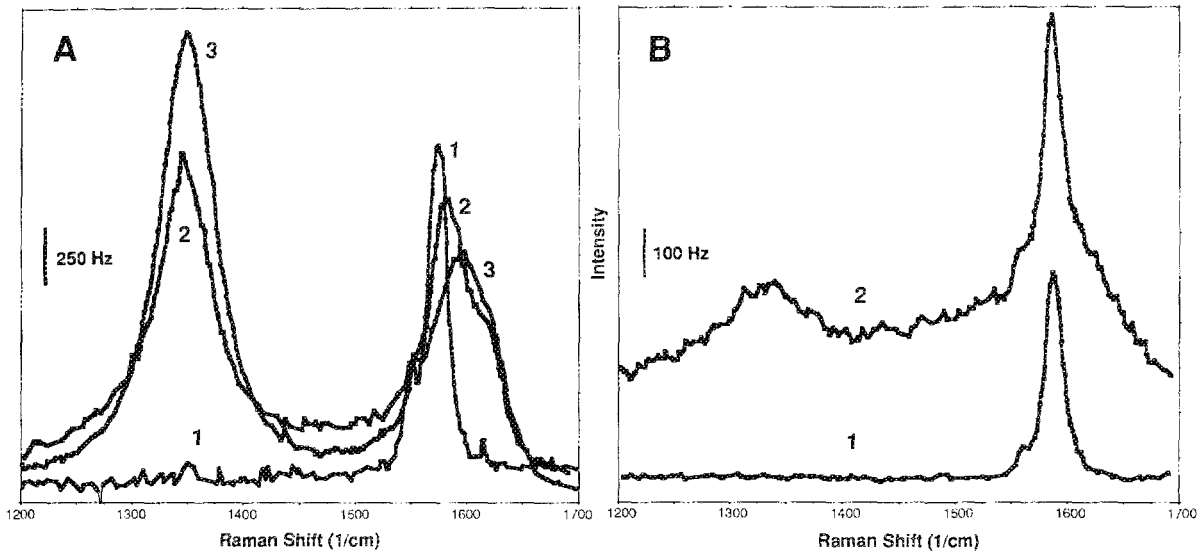

FIG. 4. Raman spectra of carbon electrode surfaces. Curves 1, 2, and 3 in (A) are of HOPG basal plane, HOPG edge plane, and glassy carbon. Curve 2 in (B) is of the laser-treated HOPG surface, while curve 1 was taken away from the laser-treated region. Adapted from Ref. 4.

For heat-treated or polished glassy carbon, $k^0_{obs} = 0.14$ cm/s, better than the laser-treated HOPG surface, improving to 0.20 cm/s after laser pulses.

Raman spectroscopy of fresh HOPG and before and after laser treatment indicates increased disorder of the laser-disrupted surfaces. Shown in Fig. 4(A) are spectra of HOPG basal and edge plane, and glassy carbon. The band at 1360 cm^{-1} is only active in crystallites of finite size,[14] and indicates the presence of significant edge plane density. The band at ~1600 cm^{-1} is complex, and is associated with interplanar bonding in graphite.[15-19] Both bands are present in the spectrum of glassy carbon; the 1360 cm^{-1} band is absent for basal plane HOPG [Fig. 4(A), curve 1], and prominent for HOPG edge plane [Fig. 4(A), curve 2]. Compared to an untreated area of HOPG [Fig. 4(B), curve 1], the spectra of the laser-damaged region shows activity at 1360 cm^{-1}, indicating increased edge plane density.

Figures 5 and 6 show STM images of HOPG following Nd:YAG (55 MW cm^{-2}) and N_2 (67 MW cm^{-2}) expo-

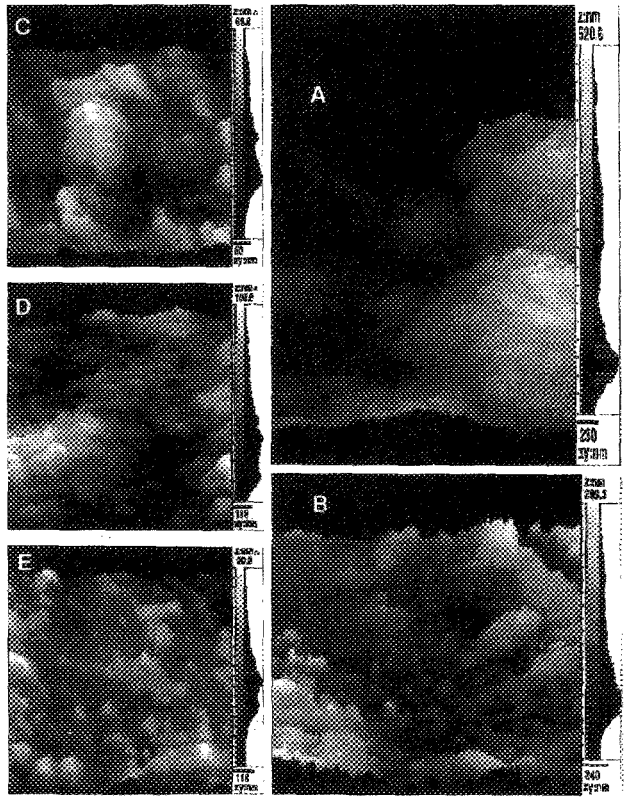

FIG. 5. STM images of the laser-treated HOPG surface, three pulses, YAG laser, 55 MW/cm^{-2}, except (B), which was at 105 MW cm^{-2}.

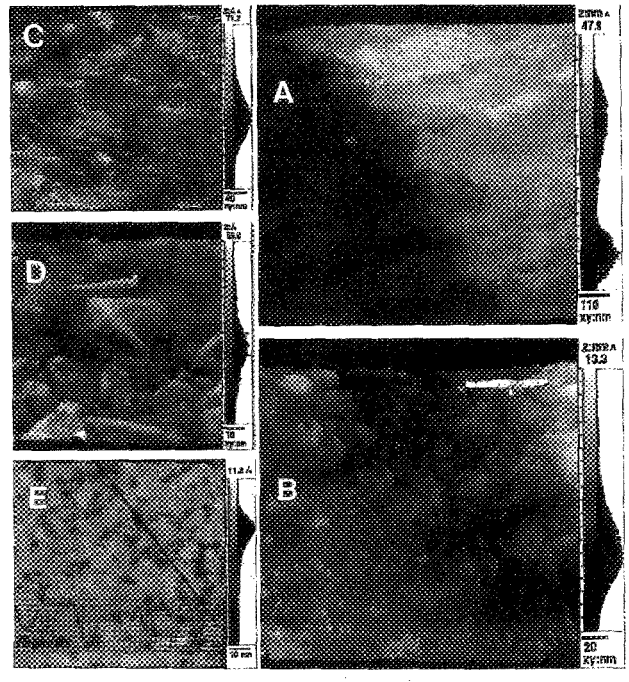

FIG. 6. STM images of laser-treated HOPG. N_2 laser, 67 MW cm^{-2}. Panel (E) shows a closeup of a smoother region with a line scan showing variations in surface height, with single- and double-monolayer pits evident.

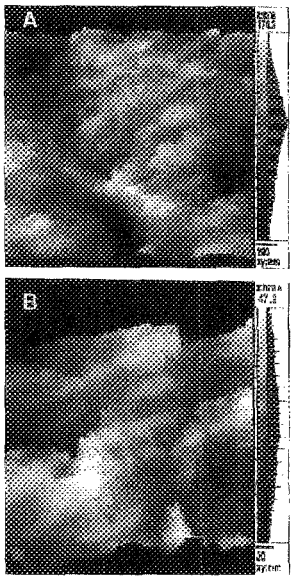

FIG. 7. STM images of laser-treated glassy carbon. YAG laser, 80 MW cm^{-2}.

sures. The basal plane surface is severely disrupted by the laser exposure. The surface roughening is extensive enough to be visible in scanning electron microscope (SEM) images,[4] which have lower resolution. Although differences in laser damage for the two lasers might be expected due to wavelength, power density, and pulse duration, these variables were not examined in detail, and the images of Figs. 5 and 6 are not sufficient to conclude any major difference between the effects of the two different lasers. STM images of the surface of glassy carbon (Fig. 7) also show increased roughening from laser pulses, even compared to the original, rough fractured surface.

IV. CONCLUSIONS

STM has been used to examine the disruption of carbon electrode surfaces resulting from irradiation with intense laser pulses. Although an exhaustive characterization of laser-generated defects was not performed, the results from two different lasers show qualitative increases in surface roughness and disorder. The STM results support spectroscopic and electrochemical measurements, indicating increased edge plane density and electrode surface area, contributing to faster observed heterogeneous electrochemical charge transfer rate constants.

[a] Authors to whom correspondence should be addressed.

[1] R. J. Rice and R. L. McCreery, Anal. Chem. **61**, 1637 (1989).
[2] I. Morcos and E. Yeager Electrochim. Acta **15**, 953 (1970).
[3] J. P. Randin and E. Yeager, J. Electroanal. Chem. **58**, 313 (1975).
[4] R. Bowling, R. Packard, and R. L. McCreery, J. Am. Chem. Soc. **111**, 1217 (1989).
[5] R. M. Wightman, M. R. Deakin, P. M. Kovach, W. G. Kuhr, and K. J. Stutts J. Electrochem. Soc. **131**, 1578 (1984).
[6] R. S. Robinson, J. Microscopy **152**, Pt2, 541 (1988).
[7] R. S. Robinson, J. Electrochem. Soc. **136**, 3145 (1989).
[8] R. S. Robinson, J. Vac. Sci. Technol. A **8**, 511 (1990).
[9] R. S. Robinson, J. Comp. Aided Microscopy **1**, 53 (1990).
[10] R. S. Robinson, T. H. Kimsey, and R. Kimsey (submitted).
[11] R. S. Robinson, T. H. Kimsey, and R. Kimsey, J. Vac. Sci. Technol. B, in press (1991).
[12] K. Sternitzke and R. L. McCreery Anal. Chem., (to be published).
[13] R. S. Robinson, K. Sternitzke, M. T. McDermott, and R. L. McCreery (submitted).
[14] F. Tuinstra and J. L. Koenig J. Chem. Phys. **53**, 1126 (1970).
[15] M. Nakamizo and K. Tamai Carbon **22**, 197 (1984).
[16] R. Tsu, J. Gonzales, and I. Hernandez, Solid State Commun. **27**, 507 (1978).
[17] M. S. Dresselhaus, and G. Dresselhaus, Adv. Phys. **30**, 139 (1981).
[18] M. Nakazimo, H. Honda, and M. Inagaki, Carbon **16**, 281 (1978).
[19] M. S. Dresselhaus and G. Dresselhaus, Adv. Phys. **30**, 290 (1981).